Tellus (1999), 51B, 734–747
Printed in UK. All rights reserved

TELLUS
ISSN 0280–6509

Air–sea CO_2 flux variability in the equatorial Pacific Ocean near 100°W

By J. ETCHETO[1]* J. BOUTIN[1], Y. DANDONNEAU[1], D. C. E. BAKKER[1], R. A. FEELY[2], R. D. LING[3], P. D. NIGHTINGALE[3] and R. WANNINKHOF[4], [1]*LODYC, UMR 7617 CNRS/ORSTOM/UPMC, Paris, France;* [2]*NOAA/PMEL, Seattle, USA;* [3]*Plymouth Marine Laboratory, Plymouth, UK;* [4]*NOAA/AOMI, Miami, USA*

(Manuscript received 27 July 1998; in final form 12 March 1999)

ABSTRACT

The interannual variability of the CO_2 partial pressure (pCO_{2oc}) in the surface layer of the east equatorial Pacific Ocean near 100°W is studied and compared with the sea surface temperature (SST) monitored from satellites. This variability is shown to be correlated with the SST anomaly rather than with the temperature itself. The pCO_{2oc} variability is related to the variability of the upwelling systems (the equatorial upwelling and the upwelling along the American coast), the main influence being from the coastal upwelling via the surface water advected from the east. A method is derived to interpolate the pCO_{2oc} measurements using the SST satellite measurements. By combining the result with the exchange coefficient (K) deduced from the wind speed provided by satellite borne instruments we deduce the air–sea CO_2 flux and for the 1st time we monitor continuously its temporal evolution. The variability of this flux is mainly due to the variability of K, with a clear seasonal variation. The flux obtained using the Liss and Merlivat (1986) relationship averaged from April 1985 to June 1997 in the region 97.5°–107.5°W 0–5°S is 1.67 mole m^{-2} yr^{-1} of CO_2 leaving the ocean with an estimated accuracy of 30%.

1. Introduction

The equatorial Pacific Ocean plays an important part in the global carbon cycle since it is the main oceanic source of carbon to the atmosphere (Tans et al., 1990). The air–sea CO_2 flux in this region is known to be very variable from year to year in association with El Niño/La Niña events (Keeling and Revelle, 1985; Feely et al., 1987; Inoue and Sugimura, 1992; Wong et al., 1993; Dandonneau, 1995; Feely et al., 1995; Wanninkhof et al., 1995). Thus, it is of particular interest to continuously monitor the air–sea CO_2 flux in this region. Due to their space and time coverage, satellite data are particularly well suited at monitoring oceanic phenomena, their drawback being that only the ocean surface can be observed. The present paper is a 1st attempt to such a monitoring of a restricted region in the equatorial east Pacific. The quantity relevant to the global carbon cycle is the air–sea CO_2 flux averaged in space and time. The CO_2 flux exchanged between ocean and atmosphere is most commonly derived from the combination of the exchange coefficient (K) with the sea to air gradient of the CO_2 partial pressure ($\Delta P = pCO_{2oc} - pCO_{2air}$). This flux is a non-linear combination of 2 variable quantities which both have to be monitored in order to derive an average flux. Our approach is to use satellite measurements as tracers of complicated oceanic processes which details we deliberately choose to ignore, our aim being to study the variability of the air–sea flux

* Corresponding author.
e-mail: je@lodyc.jussieu.fr.

of CO_2 at a large time scale and to derive its value averaged over several years.

The exchange coefficient can be deduced from the surface wind speed through a parameterization, the wind speed being a proxy to the turbulence at the air–sea interface which governs the exchange. Wind speed is monitored using the wind speed remotely sensed from satellite by microwave instruments (radars and radiometers) (Etcheto and Merlivat, 1988; Etcheto et al., 1991; Boutin and Etcheto, 1997). Several parameterizations to relate K to the surface wind speed have been proposed, based either on theoretical studies, wind tunnel and in situ measurements or on $^{14}CO_2$ inventories in the ocean. The consequences of using the different formulas are discussed in Boutin and Etcheto (1995). The effect of a possible chemical enhancement of the air–sea exchange on the results of the present study is illustrated in Boutin et al. (1999b). The air–sea CO_2 partial pressure gradient can only be measured in-situ and hence cannot be monitored continuously at large scale. In the east equatorial Pacific ocean, both K (Boutin and Etcheto, 1997) and ΔP (Dandonneau, 1995; Feely et al., 1995; Inoue and Sugimura, 1992) are highly variable. Therefore in order to compute an average air–sea CO_2 flux, the variability of K and ΔP has to be assessed. The variability of the oceanic CO_2 partial pressure (pCO_{2oc}) in the equatorial Pacific ocean has been shown to be related to the El Niño /La Niña events characterized by sea surface temperature (SST) anomalies (Inoue and Sugimura, 1992). Our approach will quantitatively relate the pCO_{2oc} variability to the SST, since SST has been continuously monitored from satellite for the last fifteen years and will continue to be. The idea behind this approach is that pCO_{2oc} in this region is mainly under the influence of the oceanic circulation, upwelling and horizontal advection, and that the SST can be used as a tracer of this circulation. The obvious limitations are that SST can be influenced by other phenomena, such as air–sea heat flux, and that the oceanic circulation not necessarily leaves an imprint on SST. Yet, the east equatorial Pacific is a region of strong upwellings (coastal and equatorial) particularly favourable to this approach. The thermodynamic effect of temperature on pCO_{2oc} is implicitly taken into account. Other phenomena, such as biology, can also influence pCO_{2oc}. Nevertheless the biology in this region is strongly influenced by oceanic circulation, and is thence partly taken into account in our approach. Since very little is known about the pCO_{2oc} variability in this region, even a crude estimate is of interest. The atmospheric CO_2 concentration is slowly variable in space and time over the ocean and it is monitored by a worldwide network so that ΔP can easily be deduced from pCO_{2oc}.

2. Data and methods

2.1. CO_2 oceanic partial pressure

Since 1991 pCO_{2oc} and ΔP have been routinely measured during the ECOA cruises along the track Panama, Mururoa, Tahiti which crosses the equatorial upwelling around 100°W; a detailed description of the ECOA experiment and results can be found in Dandonneau (1995). The measurements from a few ECOA cruises (6; 7; 12; 13) during which technical problems occurred, were discarded. An example of the measurements of pCO_{2oc} and SST made during 2 of these cruises (ECOA 3 during a warm anomaly and ECOA 14 during a cold anomaly) is shown on Fig. 1. The sharp pCO_{2oc} gradient encountered can be clearly seen, the SST gradient being less abrupt, especially in the warm case.

The cruises used are listed in Table 1: ALIZE is described in Lefevre and Dandonneau (1992); EPOCS 86 and RITS 89 in Murphy et al. (1994). The EQPAC cruises are reported by Feely et al. (1995) and Ho et al. (1997). We also use measurements made during the IRONEX 2 cruise (Cooper et al., 1996) outside the iron patch. In addition, a drifting buoy with a pCO_{2oc} sensor (CARIOCA), hereafter called CARIOPAC 1 was deployed at 100°W–1°S (see Merlivat and Brault, 1995; Hood et al., 1999, for a description) and made measurements from 29 December 1996: we use the 1st 2 weeks of measurements. The location of cruises made at constant longitude or latitude is mentioned in Table 1. The study has been made on averaged measurements in order to be representative of the region of maximum pCO_{2oc} at longitudes close to 100°W. Since pCO_{2oc} is very variable in this region (Boutin et al., 1999a), we have to define a criterium for the averaging region. Since the short scale pCO_{2oc} variations inside this area are not correlated with the wind speed variability, we may use the mean pCO_{2oc} to obtain the air–sea

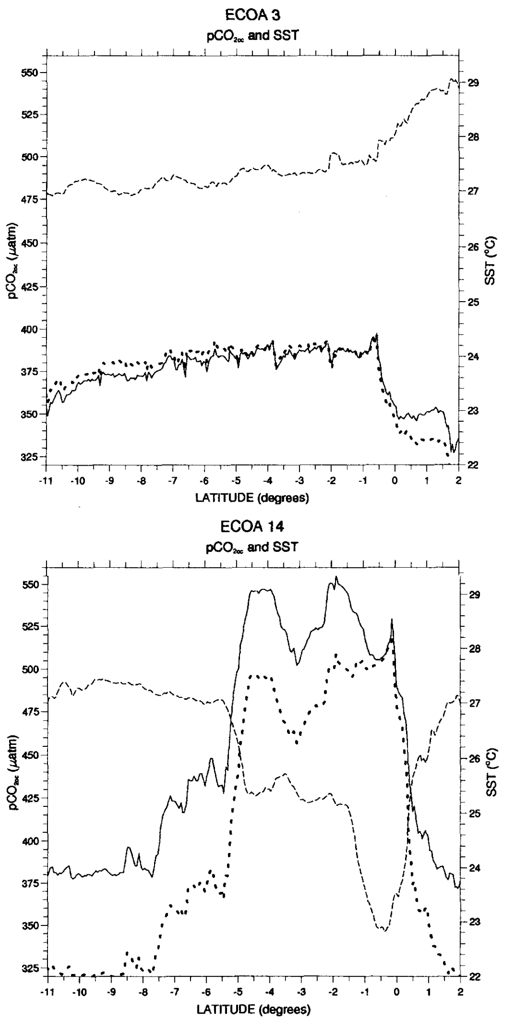

Fig. 1. pCO_{2oc} at in-situ temperature (solid line) and corrected to a constant temperature taken at 0.5°S (dotted line) and SST (dashed line): top frame during ECOA 3 (warm event); bottom frame during ECOA 14 (cold event).

Table 1. *Cruises close to 100°W*

Cruise	Date	Location
EPOCS 86	25 May 86	along equator
RITS 89	22 February 89	along 110°W
ALIZE	13 January 91	along equator
ECOA 1	14 August 91	
ECOA 2	9 November91	
ECOA 3	4 March 92	
EQPAC Spring 92	7 March 92	along 110°W
EQPAC Spring 92	14 May 92	along equator
ECOA 4	20 June 92	
ECOA 5	27 September 92	
EQPAC Fall 92	13 November 92	
EQPAC Fall 92	30 November 92	along 95°W
EQPAC Spring93	4 March 93	along 95°W
EQPAC Spring 93	10 March 93	along 110°W
ECOA 8	10 October 93	
ECOA 9	17 January 94	
EQPAC Spring 94	22 April 94	along 95°W
ECOA 10	25 April 94	
EQPAC Spring 94	13 June 94	along 95°W
EQPAC Fall 94	10 August 94	along 95°W
EQPAC Fall 94	16 August 94	along 95°W
ECOA 11	18 August 94	
EQPAC Fall 94	18 September 94	
IRONEX leg A	25 May 95	
IRONEX leg B	27 May 95	
ECOA 14	28 May 95	
IRONEX leg C	18 June 95	
ECOA 15	5 September 95	
ECOA 16	21 December 95	
ECOA 17	25 March 96	
ECOA 18	28 June 96	
ECOA 19	29 September 96	
ECOA 20	28 December 96	
CARIOPAC 1	4 January 97	

flux integrated on the region around 100°W. For the ECOA cruises, we define the limits of the average as the points on the trajectory where $pCO_{2oc} = (pCO_{2oc}$ maximum $- 10\%)$ at the closest place before and after the maximum is reached. For the examples shown in Fig. 1, the averaging zone is between 10.46°S and 0.08°S for ECOA 3 and between 4.98°S and 0.05°S for ECOA 14. The mean width of the averaging zone for the 16 ECOA cruises (hereafter called the "ECOA zone") is 5.55° latitude, between 0.25°N and 5.30°S. The corresponding longitudes are 98.1°W and 107.3°W. The average location of the maximum pCO_{2oc} is located at 1.77°S 101.7°W. This off-equator maximum is probably due to the warming of water advected from the upwelling region. The SST usually has a minimum close to the equator and increases southward as observed for ECOA 14 (Fig. 1). The maximum temperature observed in the "ECOA zone" is located at the southern edge of the zone. The mean difference between the minimum and the maximum temperature in the zone is 3.42°C, the mean difference between the northern edge of the zone and the temperature minimum is 0.39° latitude. These averages are made on 14 cruises because no temperature minimum is observed on ECOA 3 (warm event) and the minimum is outside the zone for ECOA 19 because of temporal variations. On Fig. 1, we plotted the measured pCO_{2oc} and the pCO_{2oc} corrected to the minimum temperature observed during the cruise according to the algorithm proposed by Copin-Montegut (1988, 1989). It is clear on ECOA 14 that this pCO_{2oc} at constant temperature is maximum near the equator as it is the case for most ECOA campaigns. For the non ECOA cruises, the track of the ship is very different from one cruise to another thus the method for averaging cannot be as homogeneous as it is for ECOA; yet the average should be representative of the surface pCO_{2oc} in the core of the upwelling around 100°W. For the meridional cruises we used the same criterium as for ECOA ($pCO_{2oc} > pCO_{2oc}$ max − 10%). For the cruises along the equator the data existing between 95°W and 105°W were averaged after removing measurements with high sea surface temperature (SST) and low pCO_{2oc} which are likely to be outside the upwelled waters, due to southward intrusions of north equatorial counter current water in tropical instability waves (Boutin et al., 1999a). The average, made on periods lasting from 9 h to 3 days (except for CARIOPAC 1) are dated at the middle of the averaging period. The standard deviation of the individual measurements from the average ranges from 6.5 to 18.8 μatm for the ECOA cruises (average 13.2 μatm) and from 3.5 to 18.1 μatm for the non ECOA cruises (average 9.5 μatm), 16.1 μatm for the fourteen days of CARIOPAC 1.

2.2. *Atmospheric CO_2 partial pressure*

In order to derive an air–sea flux, we need to know the air–sea CO_2 partial pressure gradient, therefore the atmospheric CO_2 partial pressure (pCO_{2air}). The CO_2 mixing ratio in dry air is deduced (P. Ciais, personal communication) from the NOAA/CMDL flasks measurements at Christmas Island (Central Pacific, 2°S) which have been smoothed in the time domain using the CCGVU procedure (Thoning et al., 1989). To infer PCO_{2air} from the CO_2 mixing ratio we compute the saturated water vapour from the SST in the zone under study ("local zone", see Subsections 2–3) using the values given by Kennish (1989). ΔP is deduced from the extrapolated pCO_{2oc} and this atmospheric partial pressure assuming a standard atmospheric pressure of 1013 mb.

2.3. *Sea surface temperature*

This study uses the global SST fields derived from the AVHRR satellite borne infrared radiometers and ship measurements by the Reynolds and Smith (1994) analysis. These weekly grids have $1° \times 1°$ spatial resolution. The estimated accuracy in the equatorial Pacific is on the order of 0.2°C (Reynolds and Smith, 1994). A weekly climatology considered as a reference is computed by averaging these fields from 1982 to 1996 (15 years) for 52 weeks in the year. Weekly anomaly grids are then obtained by subtracting the corresponding climatological grid from each original grid. The weekly temperature fields are used to compute the exchange coefficient (see Subsections 2–5) and to trace the ocean circulation. When looking at SST maps of the east equatorial Pacific (Fig. 2), it is clear that the surface water of the equatorial region near 100°W is influenced by 2 upwelling systems: the local equatorial upwelling and water from the upwelling along the south American coast advected to the northwest. Toggweiler et al. (1991) evidenced the influence of the coastal upwelling using ^{14}C measurements. The upwelling induced by the Galapagos islands does not seem to have an effect so far west. We will try to quantify the respective influence of the 2 upwellings on pCO_{2oc} by examining the SST in 2 zones, indicated by arrows on Fig. 2, chosen by looking at the SST maps: 101°W–103°W 0°S–2°S referred to as "local"; 83°W–85°W 2°S–4°S referred to as "east".

The 1st zone is representative of local events, especially the activity of the equatorial upwelling. The 2nd one represents what happens close to the American coast to water that is afterwards advected to the "ECOA zone"; it is located on the drift path of the water and close enough to the region where the water surfaced so that the upwelling SST signature is clearly visible. Fiedler (1994) studied the pigment concentration derived from the CZCS ocean color measurements: our "east" zone is on the path of water enriched in chlorophyll which can be considered as a tracer of upwelled water.

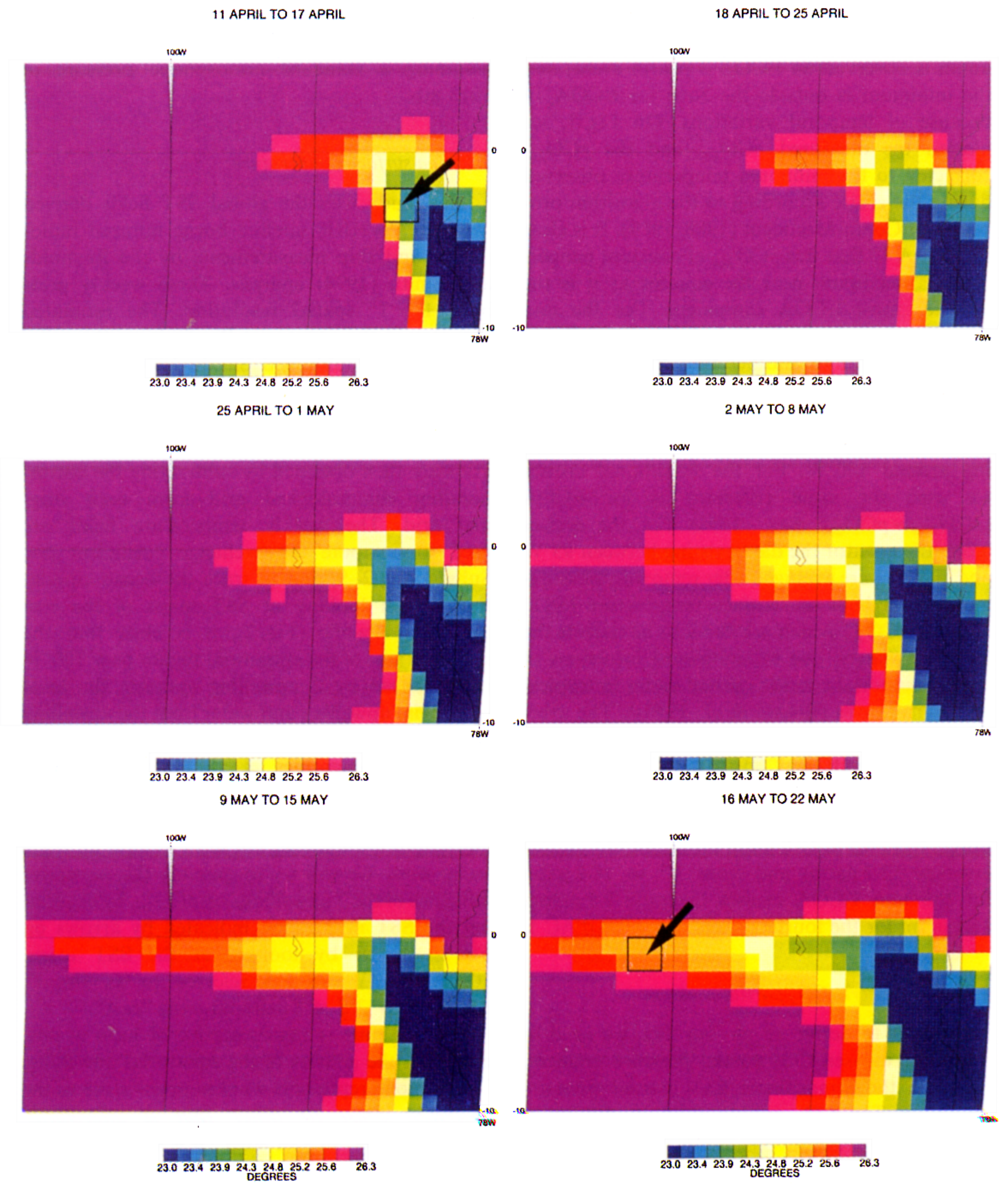

Fig. 2. SST maps of the region 78–110°W 10°S–5°N from satellite measurements for six successive climatological weeks: the path of the cold water advected from the American coast to the equatorial region can be clearly seen. The arrows in the 1st and sixth frame indicate the regions where we monitor the SST.

We will compare pCO_{2oc} with the SST anomaly in these 2 zones, with a five weeks delay for the "east zone" to take into account the time necessary for the water to be advected to the "ECOA zone".

2.4. *Exchange coefficient*

The exchange coefficient (K) is deduced from the wind speed at 10 m height above the sea surface using the Liss and Merlivat (1986) formula (Klm) and using the Wanninkhof (1992) formula (Kw). K is also slightly influenced by the sea surface temperature, varying by a few percents in the temperature range of the ocean, and this is taken into account. Each satellite wind speed measurement is converted into K. These K-values are weekly averaged in $1° \times 1°$ boxes providing weekly grids at 1° resolution. From April 1985 to January 1988, we use Geosat measurements and retrieve the wind speed at 10 m height using the Witter and Chelton (1991) algorithm; from February 1988 to July 1991 we use the SSM/I wind speeds retrieved by Wentz (1992). From August 1991 to September 1996 we use the ERS/AMI scatterometer wind speed retrieved by CERSAT/IFREMER (Quilfen and Bentamy, 1994) and from October 1996 to June 1997 we use the NASA scatterometer NSCAT. More details can be found in Boutin and Etcheto (1997).

3. Results

We will use the 16 ECOA cruises measurements to study how pCO_{2oc} relates to the SST, the 18 non ECOA cruises providing an independent verification. Before starting this study we will look at the SST anomaly in this region as a guide to the ocean circulation. In Fig. 3, the SST anomaly averaged between the equator and 2°S is plotted from 80°W to 180°W as a function of time and longitude from January 1991 to June 1997. 2 different kinds of events can be identified on this plot. The 1st category, which we interpret as an anomaly of the upwelling which develops along the American coast, starts around 85°W the cold tongue propagating toward the west, while the SST signature weakens during propagation as can be clearly seen on the six successive weekly maps of Fig. 2. This is the case of the cold events starting in March 1994, in March 1995 and in April 1996 and of the warm event starting in March 1993. The 2nd category, which we interpret as an anomaly of the large scale equatorial upwelling due to a Kelvin wave triggered by a westerly wind burst, starts in the center of the basin where the SST anomaly is maximum and propagates to the east. This is the case of the warm events starting in October 1991 and in August 1994 and of the cold event starting in September 1995. This interpretation can be checked using the sea surface height (SSH) from TOPEX/POSEIDON (not shown). While the SST signature concerns only the surface layer the SSH, in equatorial oceans, is mainly influenced by the depth of the thermocline. The anomalies of the coastal upwelling are expected to modify only a thin layer of surface water advected to the region close to the equator and should not have a signature on the SSH whereas the anomalies of the equatorial upwelling change the depth of the thermocline bringing it closer to the surface in the eastern equatorial Pacific in case of El Niño. The 1st category of events is not seen on the SSH while the 2nd category is even clearer on the SSH than on the SST proving that the 1st category concerns only a shallow surface layer of water while the 2nd category involves a much thicker layer. The eastward propagation of the phenomenon is clearly visible on the SSH, for instance for the cold event of fall 1995. While the 2nd category is considered as a modification of the equatorial upwelling and should be monitored using the local SST, the 1st one is a modification of the upwelling 15° east of the "ECOA zone", the water being advected afterwards to the "ECOA zone". To check the influence of this coastal upwelling on our pCO_{2oc} observations the scatter plot of pCO_{2oc} against the "east SST anomaly", delayed by 5 weeks to account for the advection delay is shown on Fig. 4A, while the scatter plot of pCO_{2oc} against the local SST anomaly is shown on Fig. 4B. We adjust a linear fit to the data by the least square fit method, minimizing the square of the distance of the points to the fit at a given SST.

The equation of the fit to the "east SST anomaly" is:

$$pCO_{2oc}\,(\mu\text{atm}) = 463–22.1 \text{ east SST anomaly } (°\text{C}),$$

explaining 67% of the variance. (1)

The equation of the fit to the "local SST anomaly" is:

$$pCO_{2oc}\,(\mu\text{atm}) = 460–27.4 \text{ local SST anomaly } (°\text{C}),$$

explaining 42% of the variance. (2)

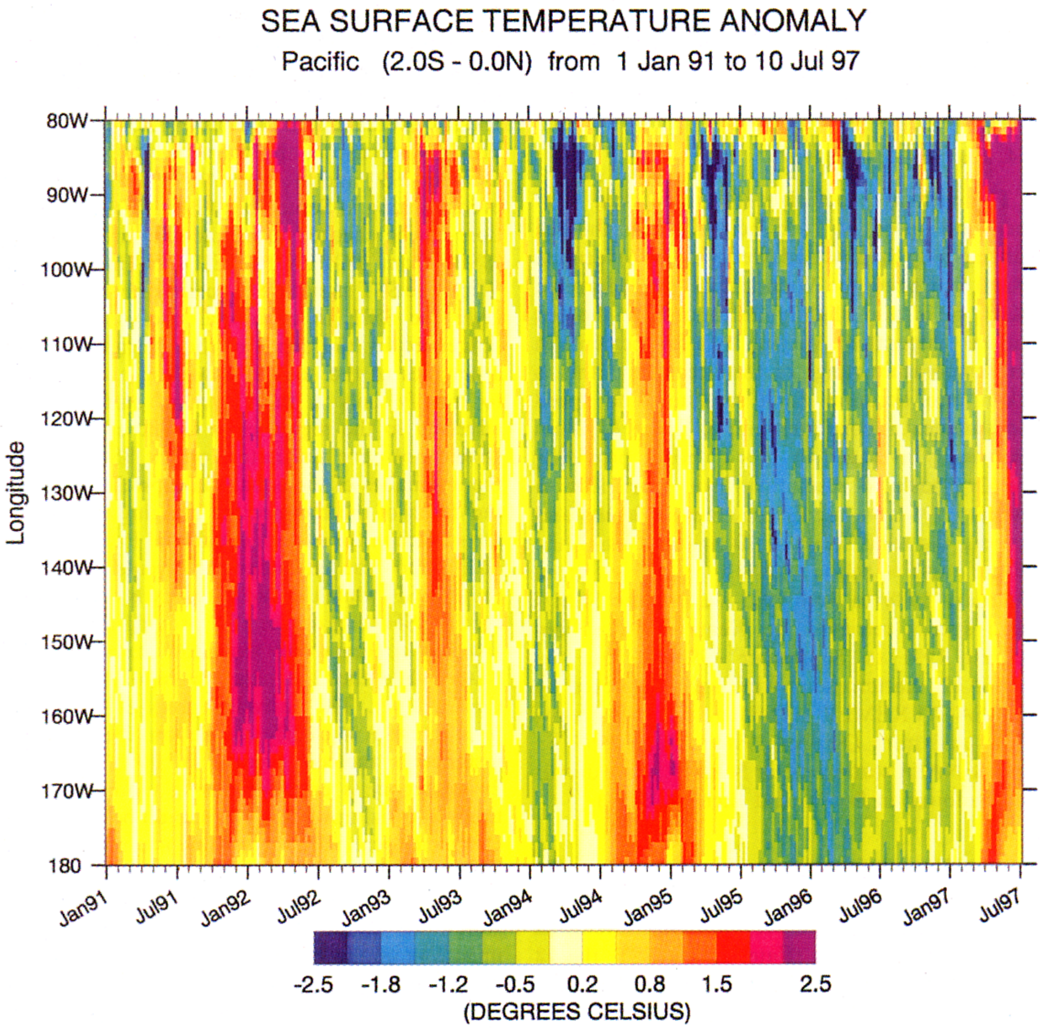

Fig. 3. Time evolution from January 1991 to June 1997 of the SST anomaly averaged between the equator and 2°S and plotted from the American coast (80°W) to the date line (180°W).

If we compare pCO_{2oc} to the local SST instead of its anomaly, the variance explained by a linear fit is only 13.6%: pCO_{2oc} is related to the SST anomaly, not to the SST itself. The SST has a strong seasonal variation: nearly 6°C between March and September; the SST anomaly retains only the interannual variability, the seasonal variation being suppressed. The lack of correlation between pCO_{2oc} and the SST, while it is much better correlated with the SST anomaly means that its seasonal variability, if any, is much weaker than its interannual variability.

The higher variance explained by eq. (1) than by eq. (2) implies that pCO_{2oc} around 100°W is mainly under the influence of water advected from the east. In order to check whether an additional local influence on pCO_{2oc} could be detected we compare the residuals of fit (1) that is [pCO_{2oc} measured] — [eq. (1)] to the "local SST" and to the "local SST anomaly". No significant correla-

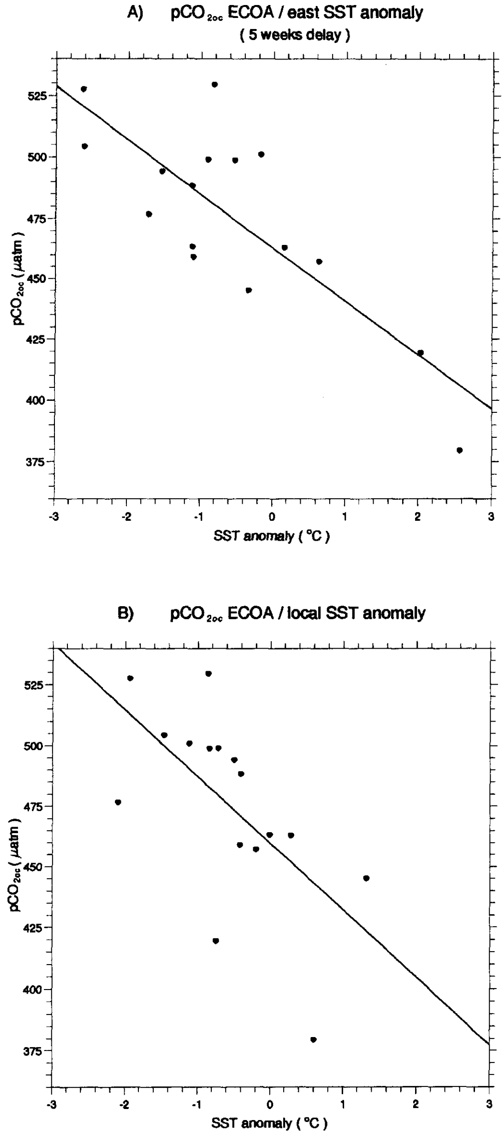

Fig. 4. Scatter plot of pCO_{2oc} against the east SST anomaly (top) and the local SST anomaly (bottom). The explained variance is respectively 67% and 42%.

tion is observed. The lack of correlation with the SST means that, even when taking into account the interannual variation of pCO_{2oc} no clear seasonal variation is observed. The lack of correlation with the "local SST anomaly" does not imply that pCO_{2oc} is not related to the local SST anomaly: the local and the east SST anomalies are strongly correlated since an anomaly of the equatorial upwelling triggered in the west Pacific propagates to the east and modifies the coastal upwelling. This can be seen from Fig. 3: the "local SST anomalies" correspond to anomalies at the eastern end of the basin while the reverse is not true, that is the "east SST anomalies" do not always correspond to "local SST anomalies", or only to weak signals. Thence once we subtracted the dependence on the east anomaly, we have also subtracted most of the dependence on the local anomaly. The root mean square deviation of the measurements with respect to the fit is 22 μatm. The results of the above study are only slightly modified if the SST smoothed over 3 weeks is used: the slope of the fit is -21.9 instead of -22.1.

If, instead of comparing pCO_{2oc} to the SST anomaly, we use the air–sea CO_2 partial pressure gradient (ΔP) we should decrease the effect of the trend due to the anthropogenic input of CO_2 since the concentration in both air and water, with a delay for the latest, is affected by a trend but we introduce a small seasonal variation originating from pCO_{2air}. The variance explained by the fit is only slightly changed: 66.5% instead of 67.1% with the east anomaly; 42.1% instead of 42.4% for the local anomaly. The corresponding fits are:

$$\Delta P\ (\mu\text{atm}) = 128–21.4 \text{ east anomaly } (°\text{C}), \quad (3)$$

$$\Delta P\ (\mu\text{atm}) = 125–26.7 \text{ local anomaly } (°\text{C}). \quad (4)$$

This study is made using the 16 ECOA campaigns. The statistical significance of such a small number of points is clearly low. Nevertheless the fact that both pCO_{2oc} and SST are deduced from a large number of points (50 to 60 measurements for pCO_{2oc}) decreases the error on the estimate of pCO_{2oc}.

The choice of a 5-week delay for the east SST anomaly has been made by examining the successive SST climatology maps shown in Fig. 2 at time when the coastal upwelling is activated by the trade winds and the progression of the cold water to the northwest can be clearly seen. It is also compatible with the results of Reverdin et al. (1994) obtained from drifters and current-meters, complemented by measurements made further east (Reverdin, personal communication). Attempts to change the delay increased the scatter of the points. Yet this delay should not be constant: it should be shorter at times of intense upwelling than at times of weak upwelling. This is not very important for our purpose (to explain the interannual variations of pCO_{2oc}): it would just introduce a 1 or 2 weeks time shift in the pCO_{2oc} retrieved using the SST, with a seasonal and interannual variation; this would not change significantly the overall result. Yet it should decrease the distance of the measurements to the fit.

In Fig. 5 top, we plotted the pCO_{2oc} calculated using eq. (1), smoothed by a running mean over 3 weeks weighted by 0.25; 0.5; 0.25 from January 1985 to June 1997. Superimposed on this curve are shown the measured pCO_{2oc}, the ECOA ones with small dots, the non ECOA ones with large dots. The error bars are the standard deviation of the measurements with respect to the average, computed for each cruise. The EPOCS 86 cruise, in May 86, is 73 μatm below the calculated value. This cruise was along the equator and measured an SST of 24.59°C averaged during the same period as pCO_{2oc} (between 95°W and 105°W). On the simultaneous SST map (not shown), the minimum SST is between the equator and 1°S, the abrupt gradient being between the raster (1°S, eq) with a SST of 24.27°C averaged on the same 10° longitude and the grid point (eq, 1°N) with a SST of 24.66°C. The equatorial measurements of the ship are thus contained between the average values south of the equator and north of the equator, closer to the northern value. In addition when the ship sailed south at 108°W, outside our averaging zone, it measured a decrease of the SST from the equator to 0.87°S, the minimum being 24.08°C. From these observations we conclude that the ship was not in the upwelling region but at its northern edge inside the SST and pCO_{2oc} gradients. Indeed for the ECOA 14 cruise (Fig. 1) it can be seen that in 0.5° latitude pCO_{2oc} varies by nearly 100 μatm while the SST changes by 1.5°C; in the same latitude interval, during ECOA 3 pCO_{2oc} varied by 40 μatm for a temperature variation of 0.4°C. Thus we interpret the large difference between EPOCS 86 and our calculated pCO_{2oc} by the fact that EPOCS 86 was outside the region we try to represent.

The comparison of non ECOA measurements with the calculated pCO_{2oc} can only be qualitative since the different cruises sampled pCO_{2oc} at different places. Yet the agreement is rather good, giving a standard deviation of the measurements (excluding EPOCS 86) to the fit of 30 μatm, especially considering that the time lag of 5 weeks is constant and does not take into account the variability of the horizontal advection in the east Pacific. In addition pCO_{2oc} is very variable in this region both in space (see Fig. 1) and in time as can be seen for instance on the 3 IRONEX legs, which took place in about 3 weeks and measured pCO_{2oc} (averaged as described in Subsection 2.1 during 19h to 36h with a standard deviation between 6.7 μatm and 15.7 μatm), differing by 7 μatm in 2 days and by 42 μatm in 22 days. Similarly ECOA 3 and EQPAC Spring 92 took place 3 days apart and differ by 17 μatm. We also find the difference of about 50 μatm between March 92 and March 93 in agreement with the measurements of Wanninkhof et al. (1996) for similar SSTs: the smoothed calculated pCO_{2oc} is 415 μatm on March 4, 1992 and 459 μatm on March 10, 1993, because a warm "east SST anomaly" was observed in February 1992 and not in February 1993.

We will now deduce the air–sea CO_2 flux (ϕ) from pCO_{2oc} computed with equation

$$\phi = K\,\Delta P. \tag{5}$$

The average of ΔP over the whole period is 125 μatm. The average pCO_{2oc} on the same period is 470 μatm. We combine the smoothed ΔP with monthly averages of K on the region 97.5–107.5°W 0–5°S assuming that the pCO_{2oc} we derive is representative of its value in this zone since its limits are very close to those of the "ECOA zone" as defined in Subsection 2.1 and that spatial variations of pCO_{2oc} inside the zone are not correlated with those of K. This is checked below. The average Klm over the whole period is 1.39×10^{-2} mole m^{-2} yr^{-1} μatm^{-1} and the average flux is 1.67 mole m^{-2} yr^{-1}. When Kw is used instead of Klm these values become 2.44×10^{-2} mole m^{-2} yr^{-1} μatm^{-1} and 2.95 mole m^{-2} yr^{-1} respectively. The assumption that ΔP and K are not correlated at shorter time scales has been checked by computing the flux during the NSCAT period (October 1996 to June 1997) with Klm and Kw averaged weakly and monthly: the result is 1.38 and 1.36 mole m^{-2} yr^{-1} respectively with Klm and 2.49 and 2.51 mole m^{-2} yr^{-1} respectively with Kw. We take into account the variations at longer time scale which could be important since the upwelling dynamics are related to the wind speed and therefore to the exchange

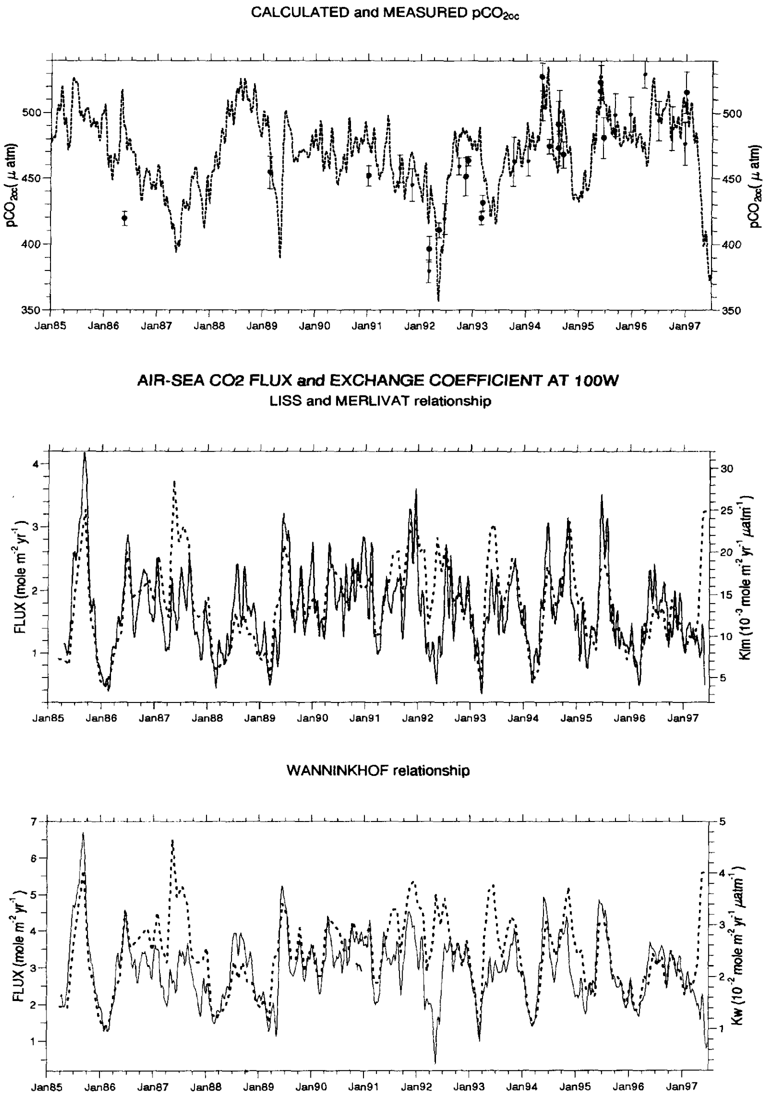

Fig. 5. Time evolution of: top panel: pCO_{2oc} computed (dashed line) and measured (ECOA cruises small dots; other cruises large dots); middle panel: exchange coefficient Klm determined from satellite measurements and the Liss and Merlivat (1986) relationship (dashed line) and air–sea CO_2 flux (solid line); bottom panel: exchange coefficient Kw determined from satellite measurements and the Wanninkhof (1992) relationship (dashed line) and air–sea CO_2 flux (solid line).

coefficient which has seasonal and interannual variations (Boutin and Etcheto, 1997). The average flux $\langle \mathrm{Klm}\Delta P \rangle$ for the whole period is 1.67 mole m^{-2} yr^{-1} while $\langle \mathrm{Klm} \rangle \cdot \langle \Delta P \rangle$ is 1.74 mole m^{-2} yr^{-1} indicating a weak correlation. The results are plotted on Fig. 5 for Klm (middle frame) and Kw (bottom frame). The flux varies between 0.4 and 4.2 mole m^{-2} yr^{-1} while the exchange coefficient varies between 0.5×10^{-2} and 2.9×10^{-2} mole m^{-1} yr^{-1} μatm^{-1}: most of the variability, mainly at seasonal scale, is due to K but pCO_{2oc} brings additional variability at interannual scale. The parametrization used to compute K is thence important not only for the average flux but also for the flux variability. This conclusion holds only for the east Pacific. As already noticed by Boutin and Etcheto (1997), the exchange coefficient has a strong seasonal variation, being minimum in March. In the eastern Pacific it tends to be large at the beginning of El Niño years, as in 1987, and low during La Niña years, as in 1988 while the contrary is true in the central Pacific. The temporal variations of the flux are mainly due to the K variability, with a clear seasonal variation except at times of low ΔP during warm events in 1987 and during the 1st half of 1992 when, even though K was larger than usual, it could not compensate the very low ΔP.

The flux values determined using Kw (Fig. 5 bottom) can be compared with the results of Feely et al. (1995), Fig. 9, and Feely et al. (1997), Fig. 6. The comparison cannot be accurate since their estimates are for a whole season with campaigns sampling different places at different dates and is derived by looking at color maps. In fall 1992 they estimate a flux of 2.7 mole $m^{-2}\,yr^{-1}$ we find 3.3, in spring 1993 they find 1.5 mole $m^{-2}\,yr^{-1}$ we find 2.2, in spring 1994 they find 2.7 mole $m^{-2}\,yr^{-1}$ we find 1.8, in fall 1994 they find 3.5 mole $m^{-2}\,yr^{-1}$ we find 3.8. For the 2 periods during which our estimate does not vary too much, fall 92 and fall 94, our estimate is above theirs but compatible, the 1994 flux being larger than the 1992 one. The difference could be due to the wind speed used to determine the flux: the ECMWF fields have been shown by Boutin et al. (1996) to be lower than the satellite measurements. This study includes their $p\mathrm{CO}_{2\mathrm{oc}}$ the differences should therefore not be due to this quantity. For spring 93 and spring 94 during which we find large fluctuations (between 1 and 3 in 93 and between 1.5 and 4.5 in 94) the difference is much larger, the 1994 flux being larger than the 1993 one for them while we find the contrary. This difference can be attributed to the undersampling of their campaigns during a period of high variability.

4. Discussion and conclusion

According to the result of the above study, the surface oceanic CO_2 concentration in the equatorial region around 100°W appears to be strongly correlated to the SST anomaly and not to the SST itself, the seasonal variation of $p\mathrm{CO}_{2\mathrm{oc}}$ is thence small as discussed in Section 3. The reason could be that the seasonal variation of the upwelling strength compensates approximately the effect of the temperature variation, with a possible additional effect of the biology: for a constant CO_2 concentration, a 6°C warming would increase $p\mathrm{CO}_{2\mathrm{oc}}$ by 120 μatm. $p\mathrm{CO}_{2\mathrm{oc}}$ in this region is dominated by water advected from the east, which influence appears to be dominant. This water is known to be cold and carbon enriched when it upwells along the American coast. Partial pressures up to 1000 μatm have been observed off the coast of Peru (Copin-Montegut and Raimbault, 1994). Since the response time to air–sea exchange is much shorter for SST than for CO_2, the thermal coastal upwelling signature disappears much faster than the CO_2 supersaturation. Thus at 100°W we still see high $p\mathrm{CO}_{2\mathrm{oc}}$ but no clear temperature anomaly. Kessler and Mc Phaden (1995) report at 140°W, 0°S a mean net air–sea heat flux of 104 W m^{-2} able to produce a SST change of about 2°C per month for a shallow mixed layer, while Hayes et al. (1991) estimate a mean net heat flux to the ocean at 110°W at the equator of 115°W m^{-2}. A 100°W m^{-2} heat flux increases the temperature of a 50 m deep mixed layer by 1.4°C in 5 weeks. The SST difference between the 2 zones used in the regression varies between 1.3°C and 2.6°C at the season of minimum SST when the upwelling activity is maximum, a value compatible with the above orders of magnitude.

While the SST signature of the water advected from the east is likely to be lost during its drift, we will estimate whether a $p\mathrm{CO}_{2\mathrm{oc}}$ signature should be kept. Lefevre et al. (1994) report a mean decrease of $p\mathrm{CO}_{2\mathrm{oc}}$ due to biology in the equatorial Pacific of 1.5 μatm day^{-1} averaged between 165°E and 95°W, while the degassing has a negligible effect (0.1 μatm day^{-1} on average, which should correspond to 0.2 μatm day^{-1} in the eastern part where the mixed layer is shallow). Since the biology is more active in the east Pacific than in the western part the biological effect could be as much as 3 μatm day^{-1}. We then estimate the decrease of $p\mathrm{CO}_{2\mathrm{oc}}$ due to biology during the 5 weeks drift of the water to be about 100 μatm. On another hand $p\mathrm{CO}_{2\mathrm{oc}}$ should be increased by the thermodynamic effect by about 40 μatm due to a 2°C warming. Another source of surface CO_2 is upwelling along the drift path of the water. The estimations of the upward velocity due to the upwelling in the equatorial east Pacific vary for different authors (Wyrtki, 1981; Halpern et al., 1989) between 1 m day^{-1} and 2.5 m day^{-1}: 2 m day^{-1} should be a reasonable estimate. The vertical gradient of the total inorganic carbon in the same region should be on the order of 1 μmol kg^{-1} m^{-1} (Wanninkof et al., 1995). Assuming a Revelle factor equal to 8.5 the increase of pCO_{2oc} due to upwelling along the drift path of the water should be about 3.9 μatm day^{-1}. We assume that upwelling along the drift path occurs only west of the Galapagos islands, corresponding to about ten days of drift. The increase of pCO_{2oc} due to upwelling is thus about 40 μatm. Combining all these estimates, we find that the pCO_{2oc} signature of the water between the "east" region where we monitor the SST and the "ECOA zone" should be modified by $-100+40+40=-20$ μatm, not enough to erase the signature of an intense upwelling. Yet the Galapagos Islands could contribute to the signature observed at 100°W but our data set does not enable us to disentangle the 2 effects. As far as the drift path and advection time of the water are concerned, they are confirmed by the trajectories of test particules in an OGCM forced by a climatological wind (Blanke, private communication). However, the measured currents have a seasonal variation (Reverdin et al., 1995) which we do not consider. Yet, since they are strong only at the time when strong upwelling brings carbon to the surface, the weakening of the currents during the warm period should not change much the results.

In order to evaluate the accuracy of our flux estimate, we consider the accuracy of ΔP to be 22 μatm, the standard deviation of the ECOA pCO_{2oc} to the fit, and the accuracy of Klm to be 1.4×10^{-3} mole m^{-2} year^{-1} μatm^{-1} according to detailed studies of the accuracy of various satellite instruments (Boutin and Etcheto, 1997), obtaining an estimate of the flux accuracy of 0.48 mole m^{-2} year^{-1},that is 30% of the total flux. When the Wanninkhof (1992) parametrization is used to compute Kw, the corresponding flux is multiplied by 1.8: this uncertainty on the flux remains in addition to the above accuracy estimate.

At last, it should be kept in mind that this study was conducted for the period 1991–1995 and is not necessarily valid for other periods, since the 90s have been reported to be different from the 80s, as far as the behavior of warm and cold events is concerned. Since very few pCO_{2oc} measurements were made prior to 1991, it is not possible to know whether the pCO_{2oc} evolution during the 80s was substantially different.

5. Acknowledgements

We thank B. Blanke for providing the results of the OPA oceanic global circulation model, P. Ciais for providing CO_2 atmospheric concentrations, M. Rafizadeh and S. Chauchereau for computing support. We are grateful to R. Cheney and the NOAA laboratory for Satellite Altimetry for providing the TOPEX-POSEIDON sea surface height measurements. This work was performed with the support of European Communities contract ENV4-CT95-0132 and of the Programme National d'Etude du Climat. The Centre National d'Etudes Spatiales provided computing time and archiving facilities.

REFERENCES

Antoine, D., Andre, J. M. and Morel, A. 1996. Oceanic primary production, 2, Estimation at global scale from satellite (coastal zone color scanner) chlorophyll. *Global Biogeochem. Cycles* **10**, 57–70.

Boutin, J. and Etcheto J. 1995. Estimating the chemical enhancement effect on the air–sea CO_2 exchange using the ERS1 scatterometer wind speeds. In: *Air–water gas transfer* (eds. Jähne, B. and Monahan, E. C.). AEON Verlag & Studio, Hanau, Germany, 827–841.

Boutin, J. and Etcheto, J. 1996. Consistency of Geosat, SSM/I and ERS1 global surface wind speeds; comparison with in-situ data. *J. Atmos. Oceanic Technol.* **13**, 183–197.

Boutin, J. and Etcheto, J. 1997. Long-term variability of the air–sea CO_2 exchange coefficient: Consequences for the CO_2 fluxes in the equatorial Pacific Ocean. *Global Biogeochem. Cycles* **11**, 453–470.

Boutin, J., Etcheto, J., Dandonneau, Y., Bakker, D. C. E., Feely, R. A., Inoue, H. Y., Ishii, M., Ling, R. D., Nightingale, P. D., Metzl, N. and Wanninkhof, R.

1999a. Satellite sea surface temperature: a powerful tool for interpreting in situ pCO_2 measurements in the equatorial Pacific Ocean. *Tellus* **B51**, in press.

Boutin, J., Etcheto, J., Emerson, S. and Ciais. P. 1999b. Possible consequences of the chemical enhancement effect for air–sea CO_2 flux estimates. *Physics and Chemistry of the Earth*, in press.

Boutin, J., Siefridt, L., Etcheto, J. and Barnier, B. 1996. Comparison of ECMWF and satellite wind speed from 1985 to 1992. *Int. J. Remote Sens.* **17**, 2897–2913.

Cooper, D. J., Watson, A. J. and Nightingale, P. D. 1996. Large decrease in ocean-surface CO_2 fugacity in response to in situ iron fertilization. *Nature* **383**, 511–513.

Copin-Montegut, C. 1988. A new formula for the effect of temperature on the partial pressure of CO_2 in seawater. *Mar. Chem.* **25**, 29–37.

Copin-Montegut, C. 1989. Corrigendum. A new formula for the effect of temperature on the partial pressure of CO_2 in seawater. *Mar. Chem.* **27**, 143–144.

Copin-Montegut, C. and Raimbault, P. 1994. The Peruvian upwelling near 15°S in August 1986. Results of continuous measurements of physical and chemical properties between 0 and 200 m depth. *Deep-Sea Res.* **41**, 439–467.

Dandonneau, Y. 1995. Sea-surface partial pressure of carbon dioxide in the eastern equatorial Pacific (August 1991 to October 1992): A multivariate analysis of physical and biological factors. *Deep-Sea Res.* **42**, 349–364.

Etcheto, J. and Merlivat, L. 1988. Satellite determination of the carbon dioxide exchange coefficient at the ocean–atmosphere interface: A first step. *J. Geophys. Res.* **93**, 15669–15678.

Etcheto, J., Boutin, J. and Merlivat, L. 1991. Seasonal variation of the CO_2 exchange coefficient over the global ocean using satellite wind speed measurements. *Tellus* **43B**, 247–255.

Feely, R. A., Gammon, R. H., Taft, B. A., Pullen, P. E., Waterman, L. S., Conway, T. J., Gendron, J. F. and Wisegarver, D. P. 1987. Distribution of chemical tracers in the eastern equatorial Pacific during and after the 1982–1983 El Niño. Southern Oscillation event. *J. Geophys. Res.* **92**, 6545–6558.

Feely, R. A., Wanninkhof, R., Costa, C. E., Murphy, P. P., Lamb, M. F. and Steckley, M. D. 1995. CO_2 distributions in the equatorial Pacific during the 1991–1992 ENSO event. *Deep-Sea Res. II* **42**, 365–386.

Feely, R. A., Wanninkhof, R., Goyet, C., Archer, D. E. and Takahashi, T. 1997. Variability of CO_2 distributions and sea–air fluxes in the central and eastern equatorial Pacific during the 1991–94 El Niño, *Deep-Sea Res.* (Part II) **44**, 1851–1868.

Fiedler, P. C. 1994. Seasonal and interannual variability of Coastal Zone Color Scanner phytoplankton pigments and winds in the eastern tropical Pacific. *J. Geophys. Res.* **99**, 18371–18384.

Halpern, D., Knox, R. A., Luther, D. S. and Philander, S. G. H. 1989. Estimates of equatorial upwelling between 140 and 110°W during 1984. *J. Geophys. Res.* **94**, 8018–8020.

Hayes, S. P., Mangum, L. J., Picaut, J., Sumi, A. and Takeuchi, K. 1991. TOGA-TAO. A moored array for real time measurements in the tropical Pacific Ocean. *Bull. Am. Meteorol. Soc.* **72**, 339–347.

Ho, D. T., Wanninkhof, R., Masters, J., Feely, R. A. and Costa, C. E. 1997. *Measurements of underway fCO_2 in the eastern equatorial Pacific on NOAA ship Malcom Baldrige and Discoverer from February to September, 1994.* NOAA Data Report AOML-30, AOML. Miami, Florida, April 1997.

Hood, E. M., Merlivat, L. and Johannessen, T. 1999. fCO_2 variations and air–sea flux of CO_2 in the Greenland Sea gyre using high-frequency time-series data from CARIOCA drift-buoys, 1999. *J. Geophys. Res.*, in press.

Inoue, H. Y. and Sugimura, Y. 1992. Variations and distributions of CO_2 in and over the equatorial Pacific during the period from the 1986/88 El Niño event to the 1988/89 La Niña event. *Tellus* **44B**, 1–22.

Keeling, C. D. and Revelle, R. 1985. Effects of El Niño.-Southern Oscillation on the atmospheric content of carbon dioxide. *Meteoritics*, **20**, 437–450.

Kennish, M. J. 1989. *Practical handbook of marine science.* 710 pp., CRC press, Florida.

Kessler, W. S. and McPhaden, M. J. 1995. The 1991–1993 El Niño in the central Pacific. *Deep- Sea Res.* **42**, 295–333.

Lefevre, N., Andrie, C., Dandonneau, Y., Reverdin, G. and Rodier, M. 1994. pCO_2, chemical properties, and estimated new production in the equatorial Pacific in January–March 1991. *J. Geophys. Res.* **99**, 12639–12654.

Lefèvre, N. and Dandonneau, Y. 1992. Air–sea CO_2 fluxes in the equatorial Pacific Ocean in January–March 1991. *Geophys. Res. Lett.* **19**, 2223–2226.

Legeckis, R. 1977. Long waves in the eastern equatorial Pacific Ocean. A view from a geostationary satellite. *Science* **197**, 1179–1181.

Liss, P. S. and Merlivat, L. 1986. Air–sea gas exchange rates: Introduction and synthesis. In: *The rôle of air–sea exchange in geochemical cycling* (ed. Buat-Ménart, P.). D. Reidel, Norwell, Mass., 113–127.

Merlivat, L. and Brault, P. 1995. Carioca buoy: carbon dioxide monitor. *Sea Technology*, October, 23–30.

Murphy, P. P., Kelly, K. C., Feely, R. A. and Gammon, R. H. 1994. *CO_2 concentrations in surface water and the atmosphere: PMEL cruises 1986–1989.* Report 1504, Pac. Mar. Environ. Lab., NOAA, Seattle, Wash., February 1994.

Quilfen, Y. and Bentamy, A. 1994. *Calibration/validation of ERS-1 scatterometer precision products.* IGARSS Proceedings, 945–947, Pasadena.

Reverdin, G., Frankignoul, C., Kestenare, E. and McPhaden, M. J. 1994. Seasonal variability in the surface currents of the equatorial Pacific. *J. Geophys. Res.* **99**, 20323–20344.

Reynolds, R. W. and Smith, T. M. 1994. Improved global

sea surface temperature analyses using optimum interpolation. *J. Clim.* **7**, 929–948.
Tans, P. P., Fung, J. Y. and Takahashi, T. 1990. Observational constraints on the global atmospheric CO_2 budget. *Science* **247**, 1431–1438.
Thoning, K., Tans, P. and Komhyr, W. 1989. Atmospheric carbon dioxide at Mauna Loa Observatory 2. Analysis of the NOAA GMCC data 1974–1985. *J. Geophys. Res.* **94**, 8549–8565.
Toggweiler, J. R., Dixon, K. and Broecker, W. S. 1991. The Peru upwelling and the ventilation of the south Pacific thermocline. *J. Geophys. Res.* **96**, 20469–20497.
Wanninkhof, R. 1992, Relationship between wind speed and gas exchange over the ocean, *J. Geophys. Res.* **97**, 7373–7382.
Wanninkhof, R., Feely, R. A., Atwood, D. K., Berberian, G., Wilson, D., Murphy, P. P. and Lamb, M. F. 1995. Seasonal and lateral variations in carbon chemistry of surface water in the eastern equatorial Pacific during 1992. *Deep-Sea Res. (II)* **42**, 387–409.
Wanninkhof, R., Feely, R. A., Chen, H., Cosca, C. and Murphy, P. P. 1996. Surface water fCO_2 in the eastern equatorial Pacific during the 1992–1993 El Niño. *J. Geophys. Res.* **101**, 16333–16343.
Wentz, F. J. 1992. Measurement of oceanic wind vector using satellite microwave radiometers, *IEEE Trans. Geosci. Remote Sens.* **30**, 960–972.
Wyrtki, K. 1981. An estimate of equatorial upwelling in the Pacific, *J. Phys. Oc.* **11**, 1205–1214.
Wong, C. S., Chang, Y. H., Smith, G. E. and Bellegay, R. D. 1993. Changes in equatorial CO_2 fluxes and new production estimated from CO_2 and nutrient levels in Pacific surface waters during the 1986/87 El Niño. *Tellus* **45B**, 64–79.